European Journal of Pharmaceutics and Biopharmaceutics 143 (2019) 8–17

Contents lists available at ScienceDirect

European Journal of Pharmaceutics and Biopharmaceutics

journal homepage: www.elsevier.com/locate/ejpb

Research paper

How does the high pressure affects the solubility of the drug within the polymer matrix in solid dispersion systems

K. Chmiel*, J. Knapik-Kowalczuk, M. Paluch

Institute of Physics, University of Silesia, ul. 75 Pułku Piechoty 1a, 41-500 Chorzów, Poland
Silesian Center for Education and Interdisciplinary Research, ul. 75 Pułku Piechoty 1a, 41-500 Chorzów, Poland

ARTICLE INFO

Keywords:
ASD
Dielectric spectroscopy
Solubility
High-pressure
Flutamide
Kollidon VA64

ABSTRACT

In this paper, we employed Broadband Dielectric Spectroscopy (BDS) in order to determine the effect of the high pressure on the solubility limits of the amorphous flutamide within Kollidon VA64 matrix. In order to achieve this goal, drug-polymer systems have been examined: (i) at ambient pressure and both isothermal and non-isothermal conditions by means of BDS as well as Differential Scanning Calorimetry (DSC), to validate proposed method; (ii) at high pressure conditions (20 and 50 MPa) and elevated temperatures (343 K, 353 K and 363 K) by means of dielectric spectroscopy. Our studies revealed that regardless of applied pressure the solubility of the flutamide within the co-polymer matrix increases with increasing temperature at isobar conditions. Moreover, our results clearly indicate that with increasing pressure the solubility of the drug within the polymer matrix is decreasing at isothermal conditions. Therefore, during the solubility limit studies one should consider the situation in which by increasing the pressure (at constant temperature) would achieve an effect similar to the lowering of the temperature (at constant pressure).

1. Introduction

Polymers in the pharmaceutical industry have a wide range of applications. The number of reports confirms their ability to increase the drug's solubility in water [1–4]. Furthermore, due to rising popularity of the extrusion-based amorphous products polymers are also used to improve both processing conditions (e.g. during Hot Melt Extrusion (HME) manufacturing) [5–7] and physical stability of the Active Pharmaceutical Ingredients (APIs) in the amorphous form [8–15]. Focusing on the latter, the source of their ability to enhance the physical stability of the amorphous materials has not yet been fully understood, except several commonly approved viewpoints. On the one hand, it is generally accepted that the capability to form drug-polymer intermolecular interactions (e.g. ionic interaction, dipole–dipole interactions or hydrogen bonding) is one of the most crucial factors during formation of the stable Amorphous Solid Dispersion (ASD) composition [16–20]. On the other hand, the addition of the polymer, characterized by glass transition temperature (T_g) higher than that of the amorphous material, will eventually increase the T_g of the system – so called antiplasticization effect – which corresponds to the reduction of the molecular mobility necessary for the cold crystallization at certain temperature [21–24]. However, above statements requires one assumption: that the two components, drug and polymer, are miscible – forms single phase, homogeneous amorphous system. This assumption is of a great significance due to the fact that thermodynamic part of the physical stability – thermodynamic stability – can be obtained only if the amount of the drug dissolved within the polymer does not exceed its solubility limits [25,26].

Over the past years the solubility of the drug molecules within the polymer matrix was one of the main concerns of the pharmaceutical scientist [27–29]. Throughout this period, time and time again researchers made discoveries revealing the true nature of this phenomenon from both experimental and theoretical point of view [30–35]. One can experimentally determine the solubility of the API-polymer ASD systems at elevated temperatures utilizing one of the methods well established in this field: (i) recrystallization method [32] (ii) melting point depression [31,33] and various annealing methods proposed throughout the years [28,36–38]. However, it has to be pointed out, that experimental determination of the solubility limits of the systems containing polymers has some limitations considering the fact that at temperatures close to or below T_g, the viscosity of this composition becomes too high to reach equilibrium state and its determination is very-time consuming [32,36,39,40]. Due to this fact numbers of analytical models were introduced in order to determine the solubility limits at lower temperatures. To this day determination of the API-polymer solubility limit can be predicted utilizing one of the following

* Corresponding author at: Institute of Physics, University of Silesia, ul. 75 Pułku Piechoty 1a, 41-500 Chorzów, Poland.
E-mail address: krzysztof.chmiel@smcebi.edu.pl (K. Chmiel).

https://doi.org/10.1016/j.ejpb.2019.08.003
Received 25 April 2019; Received in revised form 18 July 2019; Accepted 5 August 2019
Available online 06 August 2019
0939-6411/

approaches: (i) Flory-Huggins (FH) theory [30,41–44]; (ii) Hansen's solubility parameter [29,34,45]; (iii) Perturbed-Chain Statistical Associating Fluid Theory (PC-SAFT) [35,46,47].

Nevertheless, none of the aforementioned approaches considers the outcome of the applied elevated pressure on the solubility limits which is surprising since – from the experimental point of view – it would mimic manufacturing conditions i.e. tableting or HME. It has to be pointed out, however, that even though the effects of high pressure (HP) on the solubility limits has not been tested its consequence on the recrystallization tendencies of the amorphous pharmaceuticals were frequently reported. The result of enforced HP is the densification of the molecular packing of the system. This in turn leads not only to the decrease of the molecular mobility or conformational changes of molecules [48,49] but can also be a source of the improvement of drug-polymer interactions [50] or vice versa the weakening of hydrogen bonding between drug and polymer [51]. Therefore, the overall effect on the physical stability is not universal. From the one hand, one can observe the improvement of the physical stability of the amorphous materials at elevated pressure [52] yet from the other hand the escalation of the molecular packing can result in increased nucleation [53,54]. Due to this lack of unified response, the attempt to predict changes in solubility limits is extremely difficult and requires attention from the pharmaceutical point of view.

Due to the fact that dielectric spectroscopy was already employed as a technique for testing amorphous materials under the influence of high pressure [55,56] and at the same time, it has been shown recently that it can be successfully used to determine the solubility limit at ambient pressure [57–59] we decided to combine these two features in order to determine solubility limits at both elevated temperature and high pressure.

In this paper, binary amorphous mixtures of flutamide (FL) – synthetic nonsteroidal drug, currently utilized in antiandrogen therapy – and Kollidon VA64 (PVP/VA) – copolymer used widely in pharmaceutical industry – in different weight concentration were prepared by quench cooling from the melt. The aim was to determine solubility limits of FL within the PVP/VA matrix in both ambient and elevated pressure, starting from the supersaturated conditions. Thermal properties of drug-polymer systems containing different concentrations of FL and PVP/VA as well as determination of the supersaturated conditions have been investigated via Differential Scanning Calorimetry (DSC). To examine the molecular mobility, at both ambient an elevated pressure, of the investigated drug-polymer mixtures we measured them by means of Broadband Dielectric Spectroscopy (BDS). Furthermore, performed isothermal and nonisothermal measurements provide the information on the sample during recrystallization as well as allowed us to determine the concentration dependencies of the glass transition temperature of FL + PVP/VA systems. As a result of the overall BDS studies we were able to determine the solubility of the flutamide within the polymer matrix at certain temperature and certain pressure. Moreover, on the basis of DSC data, we confirmed the solubility limits determined by BDS method for ambient pressure.

2. Experimental Section

2.1. Materials

Flutamide drug of molecular mass $M_W = 276.21\ g\,mol^{-1}$ and purity ≥ 99% was purchased from Sigma-Aldrich and used as received. Kollidon VA64 – vinylpyrrolidone-vinyl acetate copolymer – (PVP/VA) of molecular mass $M_W = 45\,000–47\,000\ g\,mol^{-1}$ was purchased from BASF SE (Germany) and used as received.

2.2. Preparation of binary system

The flutamide-based amorphous solid dispersion systems were prepared at different weight concentrations of PVP/VA in each sample. To acquire homogeneous samples, we mixed compounds with polymer at appropriate ratios in mortar for approximately 20–30 min. Prepared in this way mixtures were then melted at T = 410 K – during the first DSC scan – and vitrified – by fast cooling (20 K/min) during second DSC scan – in case of calorimetric measurements. Samples preparation for the BDS and high pressure BDS measurements involved melting at T = 410 K followed by vitrification on a previously chilled copper plate. All measurements were performed immediately after preparation of the amorphous systems to avoid recrystallization.

2.3. Differential scanning calorimetry

Thermodynamic properties of FL, Kollidon VA64 and their binary systems were examined using a Mettler–Toledo DSC 1 STARe System. The measuring device was equipped with a HSS8 ceramic sensor having 120 thermocouples. The instrument was calibrated for temperature and enthalpy using indium and zinc standards. Crystallization and melting points were determined as the onset of the peak, whereas the glass transition temperature as the midpoint of the heat capacity increment. The samples were measured in an aluminum crucible (40 μL). All measurements were carried out in range from 260.15 K to 410.15 K with 10 K/min heating rate.

2.4. Broadband dielectric spectroscopy

The dielectric measurements of FL-based ASDs were carried out using Novocontrol GMBH Alpha dielectric spectrometer, in the frequency range from 10^{-1} Hz to 10^{6} Hz at temperatures from 153.15 K to 373.15 K with heating rate equal to 1 K/min. The temperature was controlled by a Quatro temperature controller with temperature stability better than 0.1 K. Dielectric studies of FL and its binary systems were performed immediately after its vitrification by fast cooling of the melt in a parallel-plate cell made of stainless steel (diameter 15 mm, and a 0.1 mm gap with quartz spacers).

For the high pressure BDS (HP BDS) measurements, we additionally employed a high pressure Unipress U111 setup. Herein, the sample was measured in a similar, made of stainless steel, parallel-plate cell (diameter of 15 mm and a 0.1 mm gap with Teflon spacers). It was sealed and mounted by a Teflon tape to separate it from the silicon liquid. Temperature was adjusted with a precision of 0.1 K by the Julabo heating circulator.

3. Results and discussion

3.1. Thermal properties of the flutamide-based ASD systems

DSC traces of the FL-PVP/VA mixtures in various weight concentrations are presented in Fig. 1. All tested mixtures are characterized by single step-like thermal event that corresponds to the glass transition. This result imply the homogeneity of the samples.[22,60] Furthermore, it has been demonstrated by Baird et al. that when the phase separation occurs, two separate thermal events (T_g) should be well visible on DSC thermogram [61]. Values of the glass transition temperature for the following compositions: FL + 55 wt% PVP/VA, FL + 41 wt% PVP/VA, FL + 27 wt% PVP/VA and FL + 13 wt% PVP/VA are equal to 326 K, 313 K, 295 K and 281 K respectively.

With increasing amount of the polymer in the mixture, the glass transition temperature of the system is rising. This common phenomenon can be easily explained by either the antiplasticization effect exerted by the addition of the polymer characterized by high T_g value or the specific interactions between components [62]. Therefore, in order to check whether or not the antiplasticization effect is dominant one should compare experimental T_g to the theoretically determined values according to the Gordon-Taylor equation [63]. It is worth mentioning that aforementioned analysis was reported recently (for different concentrations) and accordingly one can conclude that there are no

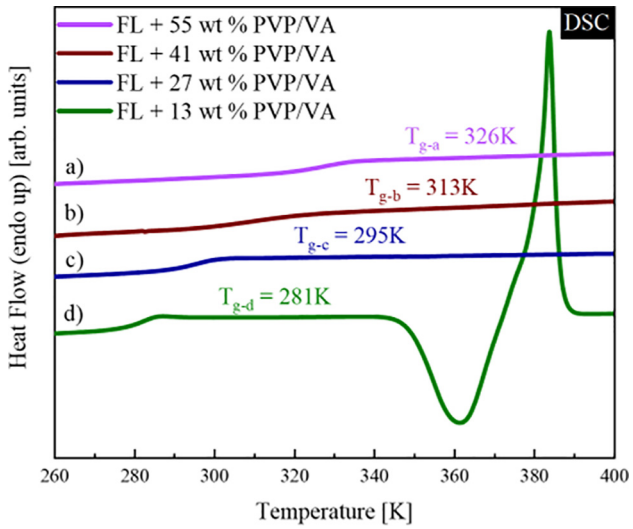

Fig. 1. Thermograms of amorphous: a) FL + 55 wt% PVP/VA (violet), b) FL + 41 wt% PVP/VA (wine), c) FL + 27 wt% PVP/VA (royal), d) FL + 13 wt% PVP/VA (green). (For interpretation of the references to colour in this figure legend, the reader is referred to the web version of this article.)

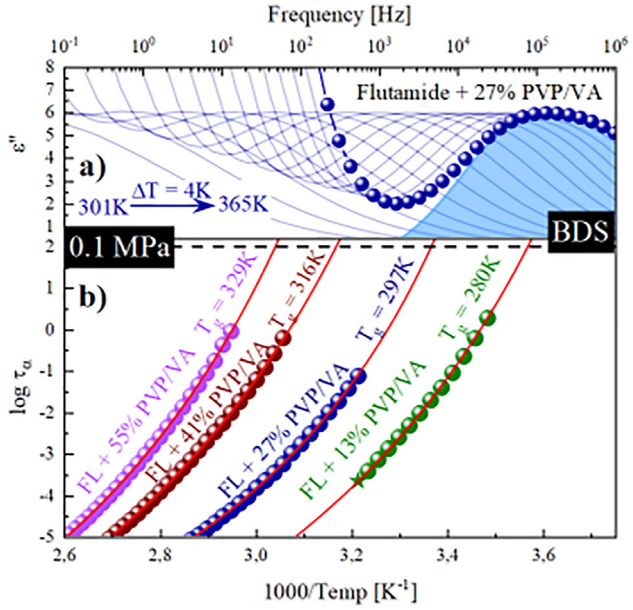

Fig. 2. Upper panel (a) presents the representative dielectric loss spectra of amorphous binary mixture of FL + 27 wt% PVP/VA above its glass transition temperature collected at ambient pressure (0.1 MPa). Royal lines indicate the α process. Blue shaded area corresponds to the fit acquired by HN function to the spectrum presented as the royal circles. Lower panel (b) shows relaxation map of binary mixtures of FL with following amount of polymer addition: 55 wt% (violet circles), 41 wt% (wine circles), 27 wt% (royal circles), 13 wt% (green circles). Star indicates the crystallization onset. Temperature dependence of τ_α in the supercooled liquid has been described by VFT equations (red solid lines). (For interpretation of the references to colour in this figure legend, the reader is referred to the web version of this article.)

significant molecular interactions between FL and PVP/VA [57]. Moreover, glass transition temperatures obtained during calorimetric measurements (see Fig. 1) were in the perfect agreement with the reported dependence (data not shown). In Fig. 1, one can observe, that during standard calorimetric measurements with heating rate of 10 K/min, samples with polymer concentration higher or equal to 27 wt% did not reveal any tendency towards recrystallization.

It has to be pointed out that the method of determination of the solubility limit used in this manuscript is built on the Mahieu's approach [32]. Method proposed by Mahieu et. al. is based on 3 steps: (i) scanning during heating of the supersaturated sample to determine initial glass transition temperature; (ii) annealing of the supersaturated sample at certain temperature; (iii) rescanning of the sample after annealing to determine the final glass transition temperature after the excess of the drug recrystallize from the solution and then identification of this newly obtained concentration by comparing its glass transition to the Gordon-Taylor prediction. Therefore, sample's tendency towards recrystallization is crucial in determination of the solubility limits. Based on the calorimetric data FL + 13 wt% PVP/VA system has the lowest physical stability (amongst tested) thus it seems to be the perfect concentration to begin the solubility limits determination. However, due to the fact that molecular dynamics was frequently found to be the crucial factor affecting physical stability of disordered pharmaceuticals, in the following Section 3.2 of this manuscript we investigated the molecular mobility of the amorphous samples via dielectric spectroscopy in order to assess their recrystallization tendencies.

3.2. Molecular dynamics studies of the flutamide-based ASDs systems at ambient pressure

In order to determine molecular dynamics of each prepared sample at ambient pressure (0.1 MPa) we performed series of BDS measurements. The representative dielectric loss spectra of FL + 27 wt% PVP/VA mixture which were obtained during heating of the amorphous sample are shown in Fig. 2a. Presented spectra exhibit one well resolved loss peak corresponding to the structural – α – relaxation. Intensity of this peak slightly decrease with the increasing temperature, as it moves towards higher frequencies. Due to the fact that no significant decrease of the dielectric strength (Δε) which corresponds to the major drop in the intensity of the structural relaxation peak – visible on dielectric loss spectra – was observed up to the 365 K, one can assume that the recrystallization process did not occur (see Fig. 2a). Considering the fact that the dielectric strength (Δε) is proportional to the number of units involved in structural relaxation, sudden drop in the intensity of the structural relaxation would reflect the onset of the sample re-crystallization [64,65]. Thus confirming that the physical stability of the sample with the PVP/VA wt. concentration equal to or higher than 27% is high enough to prevent the recrystallization process during nonisothermal experiments.

From the analysis of loss spectra recorded above the glass transition temperature we determined the temperature dependencies of the α-relaxation time for all prepared systems (see Fig. 2b). In order to obtain the values of τ_α at various temperatures, the experimental data were fitted using the Havriliak-Negami (HN) function (Eq. (1)): [66]

$$\varepsilon^*(\omega) = \varepsilon_\infty + \frac{\Delta\varepsilon}{[1 + (i\omega\tau_{HN})^a]^b} \quad (1)$$

where ε_∞ is high frequency limit permittivity, ε_0 is the permittivity of vacuum, Δε is dielectric strength, ω is equal to 2πf, τ_{HN} is the HN relaxation time, a and b represents symmetric and asymmetric broadening of relaxation peak. Representative fit of the HN function to the dielectric spectrum is presented in Fig. 2a as a blue shaded area. Using the fitting parameters determined above the values of τ_α were calculated by means of the following formula:

$$\tau_{\alpha/\alpha'} = \tau_{HN}\left[\sin\left(\frac{\pi a}{2 + 2b}\right)\right]^{\frac{1}{a}}\left[\sin\left(\frac{\pi ab}{2 + 2b}\right)\right]^{-\frac{1}{a}} \quad (2)$$

Relaxation times obtained from described above fitting procedure are presented in Fig. 2b as a filled circles. Temperature evolution of the structural relaxation time – in supercooled liquid region – usually shows non-Arrhenius like behavior. Hence, in order to parameterize it Vogel-Fulcher-Tamman (VFT) equation, that is defined as follows, was used: [67–69]

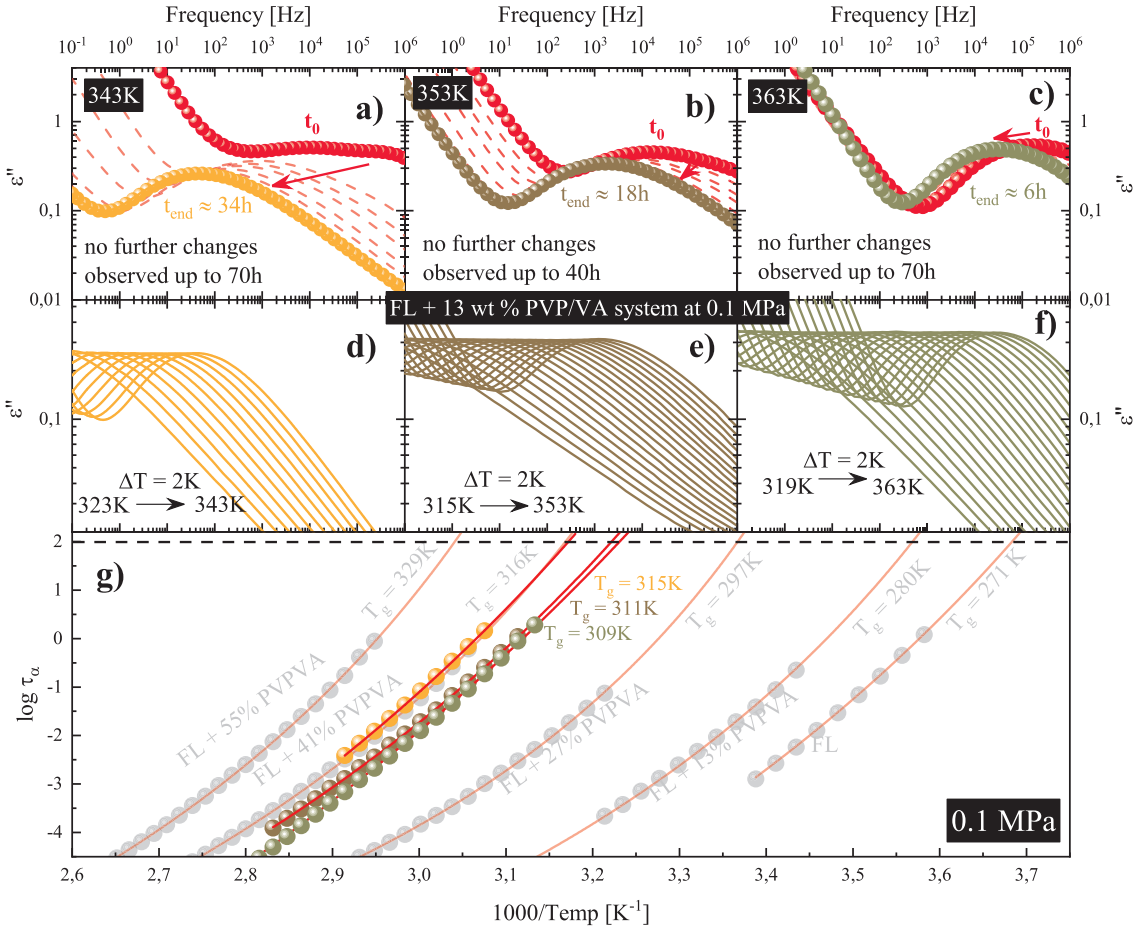

Fig. 3. Data presented in this Figure was obtained at high pressure conditions – 0.1 MPa. Upper panels: (a), (b) and (c) presents the dielectric spectra obtained during the isothermal crystallizations registered at 343 K, 353 K and 363 K respectively. t_0 indicate the first recorded spectrum at set temperature and it does not correspond to the beginning of the crystallization. Panels in the middle: (d), (e) and (f) presents dielectric spectra obtained during additional measurements performed after isothermal crystallization performed at 343 K, 353 K and 363 K as a orange, brown and dark green solid lines respectively. Lower panel (g) shows relaxation map of all binary mixtures evaluated in previous − 3.2 – sections (grey diamonds) and temperature dependence of the relaxation times registered for the samples after isothermal crystallization at 343 K, 353 K and 363 K (orange, brown and dark green circles respectively). Temperature dependence of τ_α in the supercooled liquid has been described by VFT equations (red solid lines). (For interpretation of the references to colour in this figure legend, the reader is referred to the web version of this article.)

$$\tau_\alpha(T) = \tau_\infty \exp\left(\frac{B}{T - T_0}\right) \quad (3)$$

where τ_∞, B and T_0 are the fitting parameters. To determine T_g values, we used well-known definition: $T_g = T(\tau_\alpha = 100\,s)$. Accordingly, from the extrapolation of VFT fit to 100 s we subsequently estimated T_g of FL + 55 wt% PVP/VA, FL + 41 wt% PVP/VA, FL + 27 wt% PVP/VA and FL + 13 wt% PVP/VA as 329 K, 316 K, 297 K and 280 K respectively, which is in good agreement with the calorimetric data considering different heating rate applied in both experiments. Moreover, based on the dielectric measurements, as in the case of calorimetric measurements, sample with the 13 wt% addition of the PVP/VA is the system characterized by the lowest physical stability – the greatest tendency towards recrystallization and was chosen for the solubility limit studies.

By following Mahieu's approach, one can obtain the information about the sample's concentration before and after the recrystallization and not during the whole process (excluding the possibility of rescanning the sample during the recrystallization, due to the fact that additional heating and cooling of the sample would affect the dynamic of the recrystallization process). It is worth highlighting that following the exact same procedure via BDS one can additionally obtain – aside from the initial and final glass transition temperatures – the information about the molecular dynamics of the examined system (in wide frequency and temperature range) not only before and after the recrystallization but also during the whole process. Consequently, the progress of the recrystallization as well as the exact time when this process ceased is determined considering the subtle changes in molecular dynamics. Therefore, in the following Section 3.3 of this manuscript approaches utilizing BDS and DSC (as a validation) will be employed.

3.3. Determination of the solubility limits of the FL-PVP/VA system

In order to determine the solubility limits of the FL-PVP/VA compositions series of isothermal BDS as well as DSC experiments were performed. Moreover, dielectric data, collected during measurements described in Section 3.2 of this manuscript, allowed us to establish the concentration dependency of the glass transition temperature of FL + PVP/VA systems (see Fig. 4b), which will be used to identify the concentration after the recrystallization of the excess of the API from the supersaturated sample. Based on both dielectric and calorimetric measurements, we decided, to use the sample with 13 wt% addition of polymer due to its ease of crystallization. Considering the fact that solubility limit is a function of temperature we performed isothermal measurements in three different temperatures 343 K, 353 K and 363 K (see Fig. 3a-c). One can observe in Fig. 1 that chosen temperatures are

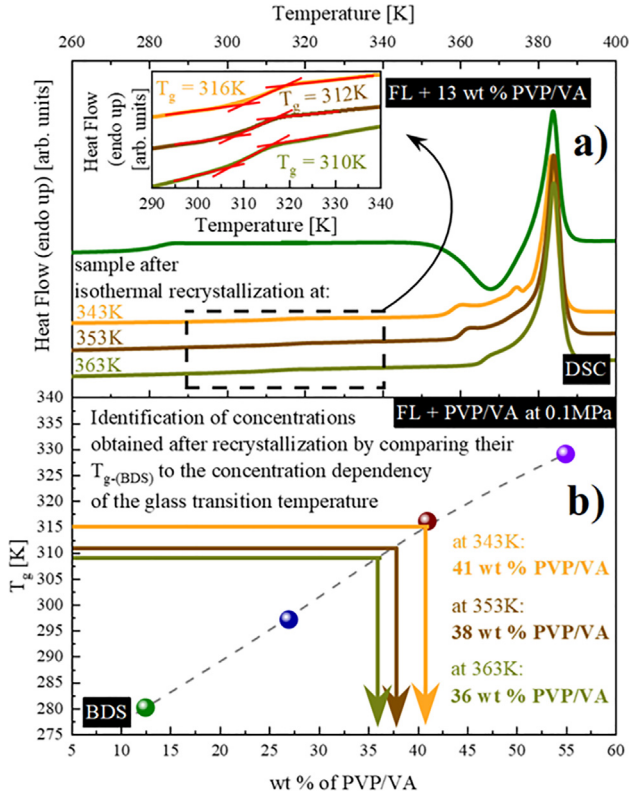

Fig. 4. Upper panel (a) presents calorimetric measurements performed after isothermal crystallization at 343 K, 353 K and 363 K. Panel a inset shows glass transitions of the systems after annealing. Lower panel (b) presents experimentally determined concentrations dependence of the glass transition temperature of the FL-PVP/VA mixtures determined by BDS measurements as well as identification of the concentration obtained after isothermal crystallization performed employing BDS.

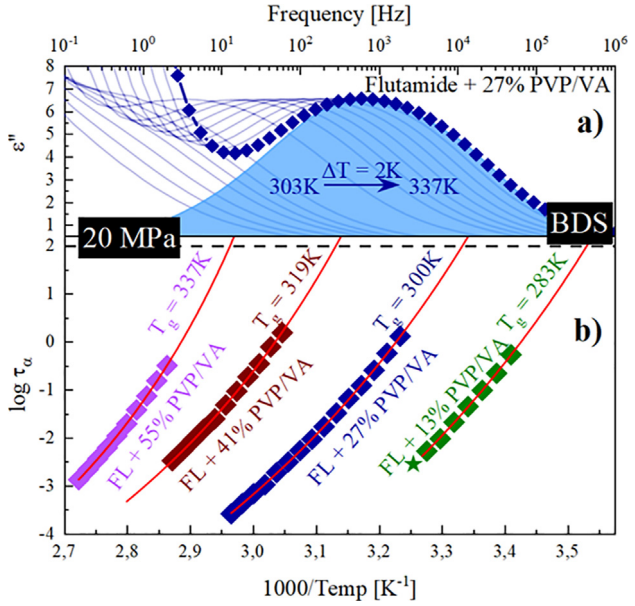

Fig. 5. Upper panel (a) presents the representative dielectric loss spectra of amorphous binary mixture of FL + 27 wt% PVP/VA above its glass transition temperature collected at elevated pressure (20 MPa). Royal lines indicate the α process. Blue shaded area corresponds to the fit acquired by HN function to the spectrum presented as the royal diamonds. Lower panel (b) shows relaxation map of binary mixtures of FL with following amount of polymer addition: 55 wt % (violet diamonds), 41 wt% (wine diamonds), 27 wt% (royal diamonds), 13 wt % (green diamonds). Star indicates the crystallization onset. Temperature dependence of τ_α in the supercooled liquid has been described by VFT equations (red solid lines). (For interpretation of the references to colour in this figure legend, the reader is referred to the web version of this article.)

still below the melting point of the system (T_m = 373 K). However, it has to be pointed out that first recorded dielectric spectrum at given temperature (marked as t_0 in Fig. 3a–c) during the isothermal experiments corresponds to the partially recrystallized sample due to the fact that onset of crystallization – based on dielectric data – is equal to 313 K (marked as a star in Fig. 2b).

When the recrystallization of the sample ended one, well resolved loss peak was still visible – α'-process (similarly to the case reported in the literature [57]). To cover wide region of relaxation times needed to determine the glass transition temperature related to the α'-process, we cooled down the sample and then measured it again on heating. During this, additional measurement the dielectric spectra of the examined samples have been registered from T = 323 K, 315 K and 319 K up to the temperature of the isothermal measurements (343 K, 353 K and 363 K respectively, see Fig. 3d–f). Points obtained from the analysis of these spectra are marked correspondingly in Fig. 3g as orange, brown and dark green circles. Once the temperature dependencies of the α'-relaxation time ($\tau_{\alpha'}$(T)), after isothermal measurements, were obtained it was possible to determine the origin of this additional process. Based on the fact that $\tau_{\alpha'}$(T) exhibits nonlinear behavior and follows VFT equation one can easily conclude that α'-process is either the primary relaxation process of different than initial concentration of FL in the FL-PVP/VA mixture or segmental relaxation of neat PVP/VA polymer, which remained amorphous after recrystallization of FL from the mixture. Extrapolation of the VFT fit to 100 s, allowed us to determine the T_g value of this additional process. Glass transition temperature values for the systems obtained after isothermal crystallization at 343 K, 353 K and 363 K are equal to 315 K, 311 K and 309 K respectively. Considering the fact that the added polymer has a T_g = 376 K [57] while

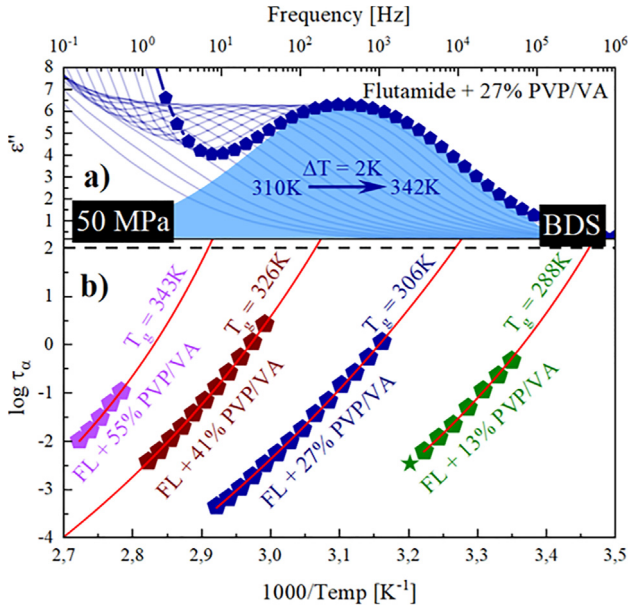

Fig. 6. Upper panel (a) presents the representative dielectric loss spectra of amorphous binary mixture of FL + 27 wt% PVP/VA above its glass transition temperature collected at elevated pressure (50 MPa). Royal lines indicate the α process. Blue shaded area corresponds to the fit acquired by HN function to the spectrum presented as the royal pentagons. Lower panel (b) shows relaxation map of binary mixtures of FL with following amount of polymer addition: 55 wt % (violet pentagons), 41 wt% (wine pentagons), 27 wt% (royal pentagons), 13 wt% (green pentagons). Star indicates the crystallization onset. Temperature dependence of τ_α in the supercooled liquid has been described by VFT equations (red solid lines). (For interpretation of the references to colour in this figure legend, the reader is referred to the web version of this article.)

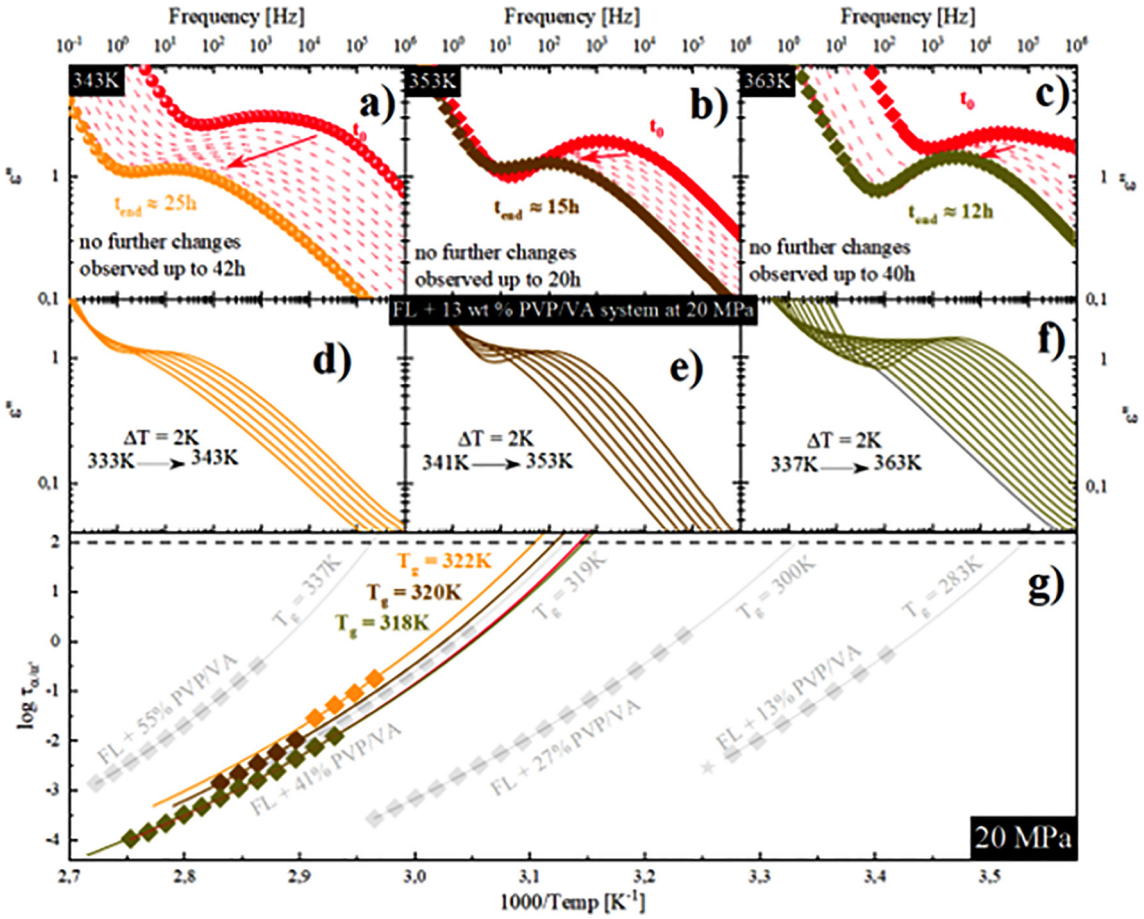

Fig. 7. Data presented in this Figure was obtained at high pressure conditions – 20 MPa. Upper panels: (a), (b) and (c) presents the dielectric spectra obtained during the isothermal crystallizations registered at 343 K, 353 K and 363 K respectively. t_0 indicate the first recorded spectrum at set temperature and it does not correspond to the beginning of the crystallization. Panels in the middle: (d), (e) and (f) presents dielectric spectra obtained during additional measurements performed after isothermal crystallization performed at 343 K, 353 K and 363 K as a orange, brown and dark green solid lines respectively. Lower panel (g) shows relaxation map of all binary mixtures evaluated in previous −3.4 – sections (grey diamonds) and temperature dependence of the relaxation times registered for the samples after isothermal crystallization at 343 K, 353 K and 363 K (orange, brown and dark green diamonds respectively). Temperature dependence of τ_α in the supercooled liquid has been described by VFT equations (red solid lines). (For interpretation of the references to colour in this figure legend, the reader is referred to the web version of this article.)

this additional process is characterized by T_g = 315 K, 311 K and 309 K respectively, one can conclude that the newly appeared process does not correspond to the segmental relaxation of the residual Kollidon VA64. Thus, confirming the initial conclusion that α'-process reflects the primary relaxation of the different than initial concentration (more detailed analysis was reported in Ref. [57]).

To validate the proposed approach, a series of calorimetric measurements were performed. During these experiments, according to the method proposed by Mahieu et al. [32], samples were annealed at 343 K, 353 K and 363 K for up to the 40 h then cooled down and scanned again during heating in order to determine the glass transition temperature (see Fig. 4a). Glass transition temperature determined after the recrystallization of the excess of the drug from the FL + 13 wt % PVP/VA mixture is equal to 316 K, 312K and 310K for annealing at 343 K, 353 K and 363 K respectively (see Fig. 4a), which is in a good agreement with the dielectric data. Once the T_g values after recrystallization were confirmed, we determined the concentrations of the corresponding mixtures by comparing these results to the experimentally determined (via BDS) concentrations dependency of the glass transition temperature of FL + PVP/VA systems (see Fig. 4b). Accordingly, one can observe in Fig. 4b that the solubility limits of the FL within the PVP/VA matrix are equal to 59 wt%, 62 wt% and 64 wt% at the 343 K, 353 K and 363 K respectively.

Our results suggest that the solubility of the drug within the polymer matrix increases with increasing temperature which follows the general trend in this kind of studies [25,32,36,70,71]. Moreover, based on presented data, BDS proved to be self-sufficient technique in terms of determining solubility limits. Additionally, this technique is commonly used to investigate the effects of the high pressure on the molecular dynamics of the glass forming liquids [52,72–75]. Therefore, we suggest utilizing BDS to assess how the high pressure affects the solubility limit of the drug within the polymer matrix (but not limited to this example) as the most suitable approach.

3.4. Molecular dynamics studies of the flutamide-based ASDs systems at elevated pressure

Similarly, to the case of measurements at ambient pressure one should start with determination of the concentrations dependencies of the glass transition temperature of FL + PVP/VA systems at each selected pressure which will enable us identification of the concentration formed after recrystallization. Therefore, in the following section of the manuscript we performed series of HP-BDS measurements, in order to determine molecular dynamics of each prepared sample as well as the solubility limits of the measured system at elevated pressure (20 and 50 MPa). The representative dielectric loss spectra of FL + 27 wt% PVP/VA mixture at 20 MPa are shown in Fig. 5a. Similarly, as in case of the 0.1 MPa dielectric loss spectra exhibit one well resolved loss peak

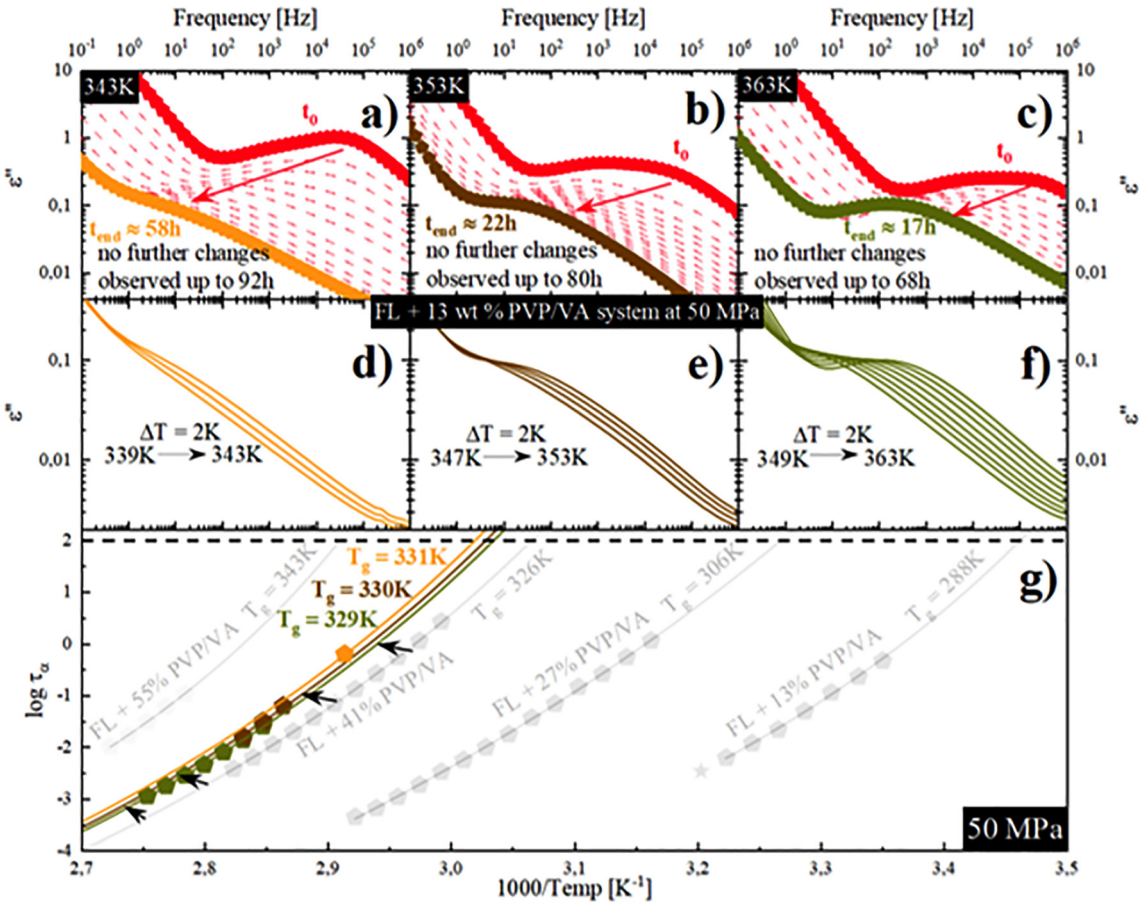

Fig. 8. Data presented in this Figure was obtained at high pressure conditions – 50 MPa. Upper panels: (a), (b) and (c) presents the dielectric spectra obtained during the isothermal crystallizations registered at 343 K, 353 K and 363 K respectively. t_0 indicate the first recorded spectrum at set temperature and it does not correspond to the beginning of the crystallization. Panels in the middle: (d), (e) and (f) presents dielectric spectra obtained during additional measurements performed after isothermal crystallization performed at 343 K, 353 K and 363 K as a orange, brown and dark green solid lines respectively. Lower panel (g) shows relaxation map of all binary mixtures evaluated in previous − 3.4 − sections (grey pentagons) and temperature dependence of the relaxation times registered for the samples after isothermal crystallization at 343 K, 353 K and 363 K (orange, brown and dark green pentagon respectively). Temperature dependence of τ_α in the supercooled liquid has been described by VFT equations (red solid lines). (For interpretation of the references to colour in this figure legend, the reader is referred to the web version of this article.)

Table 1
Glass transition temperature values for the systems obtained after isothermal crystallization of FL + 13 wt% PVP/VA sample at high pressure and elevated temperatures.

Crystallization at:	343 K	353 K	363 K
20 MPa	322 K	320 K	318 K
50 MPa	331 K	330 K	329 K

corresponding to the structural – α – relaxation which moves towards higher frequencies with increasing temperature. According to the ambient pressure, sample did not exhibit tendency towards recrystallization in examined region (see Fig. 5a). Dielectric loss spectra of fully amorphous samples, which have been registered above the glass transition temperature, were fitted by means of single HN function (see Eq. (1)). Representative fit of the HN function to the dielectric spectrum is presented in Figs. 5a and 6a as a blue shaded area.

From fitting parameters, we calculated the relaxation times of the structural relaxation of fully amorphous samples (τ_α), according to Eq. (2). In Fig. 5b one can see the temperature dependencies of τ_α marked as violet; wine; royal and green diamonds for FL + 55 wt% PVP/VA; FL + 41 wt% PVP/VA; FL + 27 wt% PVP/VA and FL + 13 wt% PVP/VA mixtures respectively. In the next step τ_α(T) dependencies were parameterize by the VFT equations. From the extrapolation of these VFT fits to τ_α = 100 s, we estimated the T_g values of the examined drug-polymer systems as follows: 337 K – 55 wt% PVP/VA; 319 K – 41 wt% PVP/VA; 300 K – 27 wt% PVP/VA and 283 K – 13 wt% PVP/VA.

Accordingly, we performed similar measurements at 50 MPa conditions (see Fig. 6). Fig. 6a presents the representative loss spectra of the FL + 27 wt% PVP/VA collected at elevated pressure – 50 MPa. Temperature dependencies of τ_α obtained from the fitting procedure of the dielectric spectra by means of HN equation (Eq. (1)) are marked in Fig. 6b as violet; wine; royal and green pentagons for FL + 55 wt% PVP/VA; FL + 41 wt% PVP/VA; FL + 27 wt% PVP/VA and FL + 13 wt % PVP/VA mixtures respectively. Next by extrapolating the VFT fits of the τ_α(T) dependences to τ_α = 100 s we determine the T_g values of the examined ASDs as follows: 343 K – 55 wt% PVP/VA; 326 K – 41 wt% PVP/VA; 306 K – 27 wt% PVP/VA and 288 K – 13 wt% PVP/VA. Obtained values of glass transition finally constitute the concentrations dependencies of the glass transition temperatures of FL + PVP/VA systems at elevated pressure: 20 MPa and 50 MPa.

3.5. Determination of the solubility limits of the FL-PVP/VA system at elevated pressure

Determination of the solubility limits was conducted similarly as at ambient pressure. We performed isothermal and isobar measurements at previously chosen: (i) temperatures: T = 343 K, T = 353 K and

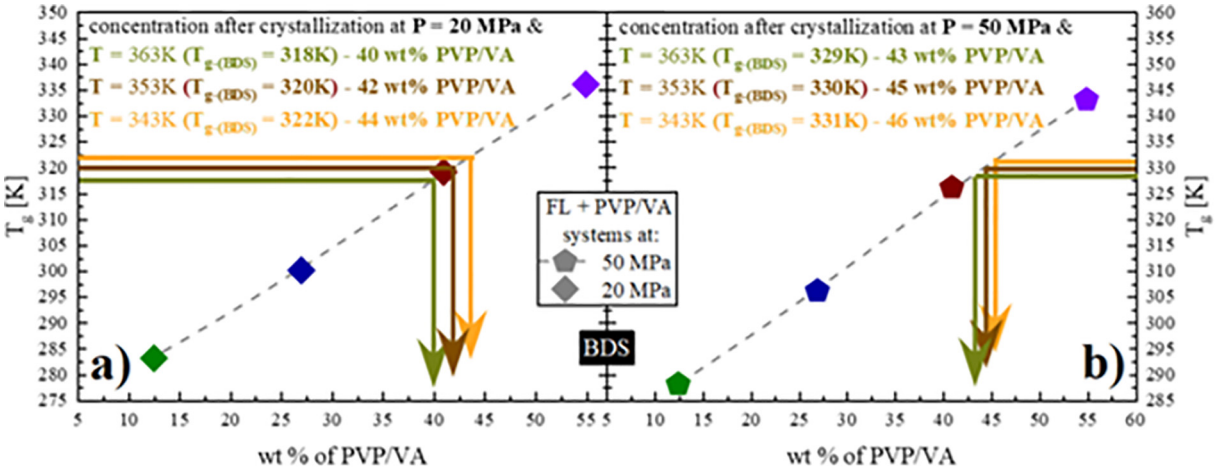

Fig. 9. Presents experimentally determined concentrations dependence of the glass transition temperature of the FL-PVP/VA mixtures at 20 MPa (a) and 50 MPa (b). Solid orange, brown and dark green lines correspond to the glass transition values after the recrystallization at isothermal – 343 K, 353 K and 363 K respectively – and isobar conditions. (For interpretation of the references to colour in this figure legend, the reader is referred to the web version of this article.)

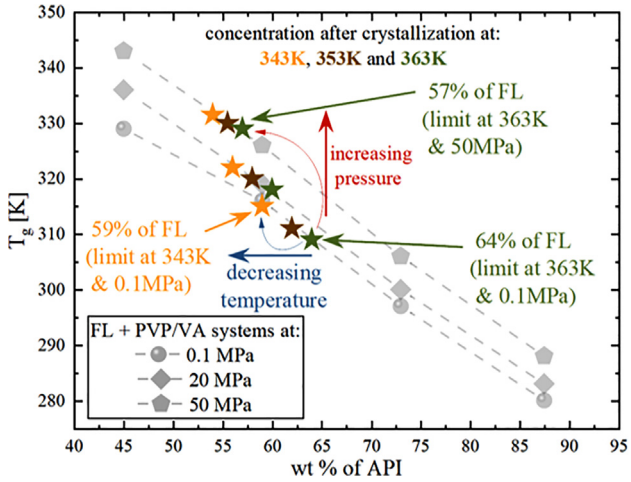

Fig. 10. Experimentally determined concentrations dependencies of the glass transition temperature of the FL-PVP/VA mixtures at 0.1 MPa, 20 MPa and 50 MPa. Orange, brown and dark green stars correspond to the concentrations obtained after the recrystallization at isothermal – 343 K, 353 K and 363 K respectively – and isobar conditions. (For interpretation of the references to colour in this figure legend, the reader is referred to the web version of this article.)

T = 363 K as well as (ii) pressure: 20 MPa (see Fig. 7) and 50 MPa (see Fig. 8). Furthermore, it has to be pointed out that – as in case of 0.1 MPa – due to the fact that onset of crystallization is equal to 307 K and 312 K for 20 MPa (marked as a star in Fig. 5b) and 50 MPa (marked as a star in Fig. 6b) respectively (based on dielectric data), first recorded dielectric spectrum at chosen pressures and temperatures (marked as t_0 in Figs. 7a–c and 8a–c) corresponds to the partially recrystallized sample.

Once the crystallizations ended one could still observe a loss peak – α'-process. To determine the relaxation times – related to the α'-process – in wide temperature range, needed to determine the glass transition temperature ($T_g = T(\tau_{\alpha'} = 100\ s)$), we cooled down the sample and then measured it again during heating. This additional procedure was conducted from 333 K, 341 K and 337 K in case of 20 MPa and from 339 K, 347 K and 349 K in case of 50 MPa, up to the temperature of the isothermal measurements – 343 K, 353 K and 363 K respectively (see Figs. 7d–f and 8d–f).

Relaxation times obtained by the analysis of these spectra are marked in Figs. 7g and 8g as orange, brown and dark green diamonds (20 MPa) and pentagons (50 MPa). In both cases of elevated pressure – besides the recrystallization at 20 MPa and 363 K – the number of the experimentally determined relaxation times after recrystallization is not sufficient in order to parameterize it well with the VFT equation. However, due to the fact that obtained relaxation times are in close proximity to well-parameterized data of FL + 41 wt% PVP/VA (see Figs. 7g and 8g), we decided to use this extrapolation of the VFT and transfer it horizontally to match the obtained points (orange, brown and dark green lines in Figs. 7g and 8g). This approach was validated in case of the points obtained after the recrystallization at 20 MPa and 363 K. As can be seen in the Fig. 7g, the horizontally transferred fit (dark green line) is in very good agreement with the VFT fit of the experimental points (red line).

Determined values of the glass transition temperature for the systems obtained after isothermal crystallization at high pressure are collected in Table 1.

Based on the dielectric measurements described in Section 3.4 of this manuscript, we were able to determine concentrations dependencies of the glass transition temperatures at elevated pressure (see Fig. 9a and b). Furthermore, one can identify the newly obtained concentration (solubility limit at certain temperature and certain pressure) by comparing determined T_g values to the presented in Fig. 9a and b dependencies.

The solubility of the investigated drug within the polymer, increases with increasing temperature, at isobar conditions – regardless of applied pressure (see Fig. 9). However, it is worth highlighting, that mentioned solubility is decreasing with increasing pressure at isothermal conditions. It has to be pointed out that observed phenomenon suggest that increase of the pressure at isothermal conditions gives similar results as the decrease of the temperature under the same pressure (see Fig. 10). Thus, the correlation between the pressure and the temperature during solubility limit studies can be presented as the $p = 1/T$.

These results are of a great importance from the pharmaceutical industry point of view. Considering the increasing popularity of the extrusion-based amorphous products, one has to acknowledge the fact that due to the increased pressure, while the system is passing through the dies, API can partially recrystallize. Formed crystallites, in turn, can affect the viscosity of the system what might eventually disrupt the extrusion process. This conclusion, however, still needs further exploration.

4. Conclusions

In this article we employed dielectric spectroscopy in order to

determine the effect of high-pressure on the solubility limits of the API-polymer systems. It is, to the best of our knowledge, the first time when dielectric spectroscopy was used for this purpose. Throughout our studies on the example of flutamide we confirmed that utilizing BDS provides the results that are in very good agreement to those obtained via DSC measurements in case of determining solubility limits. Moreover, due to the fact that one can determine the glass transition temperature using dielectric spectroscopy ($T_g = T(\tau_\alpha = 100\,s)$) as well as monitor in the real-time changes occurring in the molecular mobility during recrystallization of the sample, this technique proved to be self-sufficient in aforementioned solubility studies. Obtained results indicate that with increasing pressure (from 0.1 MPa to 20 MPa and 50 MPa) the solubility of the FL within PVP/VA matrix is decreasing at isothermal conditions (64, 60 and 57 wt% of FL at 363 K; 62, 58 and 55 wt% of FL at 353 K; 59, 56 and 54 wt% of FL at 343 K respectively). Therefore, during the solubility limit studies one should consider the fact that increasing the pressure – at constant temperature – would result in effect similar to the lowering of the temperature – at constant pressure.

We acknowledge the fact that utilizing BDS in these particular studies requires additional investigation; however, due to its ease of use, we believe that this method become an irreplaceable tool for the determination of the high-pressure solubility limits

Acknowledgement

The authors, K.C. and M.P., are grateful for the financial support received within the Project No. 2015/16/W/NZ7/00404 (SYMFONIA 3) from the National Science Centre, Poland. Additionally, the authors wish to thank Urszula Chmiel for her help with the TOC graphics preparation.

References

[1] J. Knapik, Z. Wojnarowska, K. Grzybowska, L. Hawelek, W. Sawicki, K. Wlodarski, J. Markowski, M. Paluch, Physical stability of the amorphous anticholesterol agent (Ezetimibe): the role of molecular mobility, Mol. Pharm. 11 (2014) 4280–4290, https://doi.org/10.1021/mp500498e.

[2] N. Ogawa, T. Hiramatsu, R. Suzuki, R. Okamoto, K. Shibagaki, K. Fujita, C. Takahashi, Y. Kawashima, H. Yamamoto, Improvement in the water solubility of drugs with a solid dispersion system by spray drying and hot-melt extrusion with using the amphiphilic polyvinyl caprolactam-polyvinyl acetate-polyethylene glycol graft copolymer and d-mannitol, Eur. J. Pharm. Sci. 111 (2018) 205–214, https://doi.org/10.1016/J.EJPS.2017.09.014.

[3] M.A. Altamimi, S.H. Neau, A study to identify the contribution of Soluplus® component homopolymers to the solubilization of nifedipine and sulfamethoxazole using the melting point depression method, Powder Technol. 338 (2018) 576–585, https://doi.org/10.1016/J.POWTEC.2018.07.027.

[4] J. Szafraniec, A. Antosik, J. Knapik-Kowalczuk, K. Chmiel, M. Kurek, K. Gawlak, M. Paluch, R. Jachowicz, Enhanced dissolution of solid dispersions containing bicalutamide subjected to mechanical stress, Int. J. Pharm. 542 (2018), https://doi.org/10.1016/j.ijpharm.2018.02.040.

[5] J. Aho, M. Edinger, J. Botker, S. Baldursdottir, J. Rantanen, Oscillatory shear rheology in examining the drug-polymer interactions relevant in hot melt extrusion, J. Pharm. Sci. 105 (2016) 160–167, https://doi.org/10.1016/J.XPHS.2015.11.029.

[6] F. Yang, Y. Su, J. Zhang, J. DiNunzio, A. Leone, C. Huang, C.D. Brown, Rheology guided rational selection of processing temperature to prepare copovidone-nifedipine amorphous solid dispersions via hot melt extrusion (HME), Mol. Pharm. 13 (2016) 3494–3505, https://doi.org/10.1021/acs.molpharmaceut.6b00516.

[7] M.A. Repka, T.G. Gerding, S.L. Repka, J.W. McGinity, Influence of plasticizers and drugs on the physical-mechanical properties of hydroxypropylcellulose films prepared by hot melt extrusion, Drug Dev. Ind. Pharm. 25 (1999) 625–633, https://doi.org/10.1081/DDC-100102218.

[8] S. Mohapatra, S. Samanta, K. Kothari, P. Mistry, R. Suryanarayanan, Effect of polymer molecular weight on the crystallization behavior of indomethacin amorphous solid dispersions, Cryst. Growth Des. 17 (2017) 3142–3150, https://doi.org/10.1021/acs.cgd.7b00096.

[9] P. Mistry, K.K. Amponsah-Efah, R. Suryanarayanan, Rapid assessment of the physical stability of amorphous solid dispersions, Cryst. Growth Des. 17 (2017) 2478–2485, https://doi.org/10.1021/acs.cgd.6b01901.

[10] K. Grzybowska, K. Chmiel, J. Knapik-Kowalczuk, A. Grzybowski, K. Jurkiewicz, M. Paluch, Molecular factors governing the liquid and glassy states recrystallization of celecoxib in binary mixtures with excipients of different molecular weights, Mol. Pharm. 14 (2017) 1154–1168, https://doi.org/10.1021/acs.molpharmaceut.6b01056.

[11] H. Mesallati, L. Tajber, Polymer/amorphous salt solid dispersions of ciprofloxacin, Pharm. Res. 34 (2017) 2425–2439, https://doi.org/10.1007/s11095-017-2250-z.

[12] S. Baghel, H. Cathcart, N.J. O'Reilly, Polymeric amorphous solid dispersions: a review of amorphization, crystallization, stabilization, solid-state characterization, and aqueous solubilization of biopharmaceutical classification system class II drugs, J. Pharm. Sci. 105 (2016) 2527–2544, https://doi.org/10.1016/j.xphs.2015.10.008.

[13] K. Grzybowska, S. Capaccioli, M. Paluch, Recent developments in the experimental investigations of relaxations in pharmaceuticals by dielectric techniques at ambient and elevated pressure, Adv. Drug Deliv. Rev. 100 (2016) 158–182, https://doi.org/10.1016/j.addr.2015.12.008.

[14] R. Laitinen, K. Löbmann, C.J. Strachan, H. Grohganz, T. Rades, Emerging trends in the stabilization of amorphous drugs, Int. J. Pharm. 453 (2013) 65–79, https://doi.org/10.1016/j.ijpharm.2012.04.066.

[15] J. Szafraniec, A. Antosik, J. Knapik-Kowalczuk, M. Kurek, K. Syrek, K. Chmiel, M. Paluch, R. Jachowicz, Planetary ball milling and supercritical fluid technology as a way to enhance dissolution of bicalutamide, Int. J. Pharm. 533 (2017) 470–479 https://www.sciencedirect.com/science/article/pii/S037851731730265X (accessed January 14, 2019).

[16] L.S. Taylor, G. Zografi, Spectroscopic characterization of interactions between PVP and indomethacin in amorphous molecular dispersions, Pharm. Res. 14 (1997) 1691–1698, https://doi.org/10.1023/A:1012167410376.

[17] M.M. Knopp, J.H. Nguyen, C. Becker, N.M. Francke, E.B. Jørgensen, P. Holm, R. Holm, H. Mu, T. Rades, P. Langguth, Influence of polymer molecular weight on in vitro dissolution behavior and in vivo performance of celecoxib:PVP amorphous solid dispersions, Eur. J. Pharm. Biopharm. 101 (2016) 145–151, https://doi.org/10.1016/j.ejpb.2016.02.007.

[18] A.C.F. Rumondor, L.A. Stanford, L.S. Taylor, Effects of polymer type and storage relative humidity on the kinetics of felodipine crystallization from amorphous solid dispersions, Pharm. Res. 26 (2009) 2599–2606, https://doi.org/10.1007/s11095-009-9974-3.

[19] A.C.F. Rumondor, I. Ivanisevic, S. Bates, D.E. Alonzo, L.S. Taylor, Evaluation of drug-polymer miscibility in amorphous solid dispersion systems, Pharm. Res. 26 (2009) 2523–2534, https://doi.org/10.1007/s11095-009-9970-7.

[20] P. Mistry, R. Suryanarayanan, Strength of drug-polymer interactions: implications for crystallization in dispersions, Cryst. Growth Des. 16 (2016) 5141–5149, https://doi.org/10.1021/acs.cgd.6b00714.

[21] B.C. Hancock, S.L. Shamblin, G. Zografi, Molecular mobility of amorphous pharmaceutical solids below their glass transition temperatures, Pharm. Res. 12 (1995) 799–806, https://doi.org/10.1023/A:1016292416526.

[22] J. Knapik, Z. Wojnarowska, K. Grzybowska, K. Jurkiewicz, L. Tajber, M. Paluch, Molecular dynamics and physical stability of coamorphous ezetimib and indapamide mixtures, Mol. Pharm. 12 (2015) 3610–3619, https://doi.org/10.1021/acs.molpharmaceut.5b00334.

[23] J. Knapik-Kowalczuk, W. Tu, K. Chmiel, M. Rams-Baron, M. Paluch, Co-stabilization of amorphous pharmaceuticals - the case of nifedipine and nimodipine, Mol. Pharm. 15 (2018), https://doi.org/10.1021/acs.molpharmaceut.8b00308.

[24] M.H. Fung, R. Suryanarayanan, Use of a plasticizer for physical stability prediction of amorphous solid dispersions, Cryst. Growth Des. 17 (2017) 4325, https://doi.org/10.1021/acs.cgd.7b00625.

[25] Y. Tian, J. Booth, E. Meehan, D.S. Jones, S. Li, G.P. Andrews, Construction of drug-polymer thermodynamic phase diagrams using flory-huggins interaction theory: identifying the relevance of temperature and drug weight fraction to phase separation within solid dispersions, Mol. Pharm. 10 (2013) 236–248, https://doi.org/10.1021/mp300386v.

[26] K. Lehmkemper, S.O. Kyerematen, M. Bartels, M. Degenhardt, G. Sadowski, Physical stability of API/polymer-blend amorphous solid dispersions, Eur. J. Pharm. Biopharm. 124 (2018) 147–157, https://doi.org/10.1016/J.EJPB.2017.12.002.

[27] G.W.H. Höhne, W.F. Hemminger, H.-J. Flammersheim, Differential Scanning Calorimetry, Springer Berlin Heidelberg, Berlin, Heidelberg, 2003, https://doi.org/10.1007/978-3-662-06710-9.

[28] R.E. Tamagawa, W. Martins, S. Derenzo, A. Bernardo, M.P. Rolemberg, P. Carvan, M. Giulietti, Short-cut method to predict the solubility of organic molecules in aqueous and nonaqueous solutions by differential scanning calorimetry, Cryst. Growth Des. 6 (2006) 313–320, https://doi.org/10.1021/cg050128y.

[29] P.J. Marsac, T. Li, L.S. Taylor, Estimation of drug-polymer miscibility and solubility in amorphous solid dispersions using experimentally determined interaction parameters, Pharm. Res. 26 (2009) 139–151, https://doi.org/10.1007/s11095-008-9721-1.

[30] P.J. Flory, Thermodynamics of high polymer solutions, J. Chem. Phys. 10 (1942) 51–61, https://doi.org/10.1063/1.1723621.

[31] P.J. Flory, Principles of Polymer Chemistry, Cornell University Press, 1953 https://books.google.pl/books/about/Principles_of_Polymer_Chemistry.html?id=CQ0EbEkT5R0C&redir_esc=y (accessed March 4, 2019).

[32] A. Mahieu, J.-F. Willart, E. Dudognon, F. Danède, M. Descamps, A new protocol to determine the solubility of drugs into polymer matrixes, Mol. Pharm. 10 (2013) 560–566, https://doi.org/10.1021/mp3002254.

[33] T. Nishi, T.T. Wang, Melting point depression and kinetic effects of cooling on crystallization in poly(vinylidene fluoride)-poly(methyl methacrylate) mixtures, Macromolecules. 8 (1975) 909–915, https://doi.org/10.1021/ma60048a040.

[34] C.M. Hansen, The three-dimensional solubility parameter - key to paint component affinities: solvents, plasticizers, polymers, and resins. II. Dyes, emulsifiers, mutual solubility and compatibility, and pigments III Independent calculation of the parameter components, J. Paint Technol. 39 (1967) 505–510 http://www.bcin.ca/bcin/detail.app?id=51777 (accessed January 8, 2019).

[35] J. Gross, G. Sadowski, Perturbed-chain SAFT: an equation of state based on a

perturbation theory for chain molecules, Ind. Eng. Chem. Res. 40 (2001) 1244–1260, https://doi.org/10.1021/ie0003887.
[36] Y. Sun, J. Tao, G.G.Z. Zhang, L. Yu, Solubilities of crystalline drugs in polymers: an improved analytical method and comparison of solubilities of indomethacin and nifedipine in PVP, PVP/VA, and PVAc, J. Pharm. Sci. 99 (2010) 4023–4031, https://doi.org/10.1002/jps.22251.
[37] R. Mohan, H. Lorenz, A.S. Myerson, Solubility measurement using differential scanning calorimetry, Ind. Eng. Chem. Res. 41 (2002) 4854–4862, https://doi.org/10.1021/ie0200353.
[38] K. Park, J.M.B. Evans, A.S. Myerson, Determination of solubility of polymorphs using differential scanning calorimetry, Cryst. Growth Des. 3 (2003) 991–995, https://doi.org/10.1021/cg0340502.
[39] F. Qian, J. Huang, M.A. Hussain, Drug-polymer solubility and miscibility: stability consideration and practical challenges in amorphous solid dispersion development, J. Pharm. Sci. 99 (2010) 2941–2947, https://doi.org/10.1002/jps.22074.
[40] J. Tao, Y. Sun, G.G.Z. Zhang, L. Yu, Solubility of small-molecule crystals in polymers: D-Mannitol in PVP, indomethacin in PVP/VA, and nifedipine in PVP/VA, Pharm. Res. 26 (2009) 855–864, https://doi.org/10.1007/s11095-008-9784-z.
[41] Y. Zhao, P. Inbar, H.P. Chokshi, A.W. Malick, D.S. Choi, Prediction of the thermal phase diagram of amorphous solid dispersions by flory-huggins theory, J. Pharm. Sci. 100 (2011) 3196–3207, https://doi.org/10.1002/jps.22541.
[42] A. Kozyra, N.A. Mugheirbi, K.J. Paluch, G. Garbacz, L. Tajber, Phase diagrams of polymer-dispersed liquid crystal systems of itraconazole/component immiscibility induced by molecular anisotropy, Mol. Pharm. (2018), https://doi.org/10.1021/acs.molpharmaceut.8b00724.
[43] C.B. Potter, M.T. Davis, A.B. Albadarin, G.M. Walker, Investigation of the dependence of the Flory-Huggins interaction parameter on temperature and composition in a drug-polymer system, Mol. Pharm. 15 (2018) 5327–5335, https://doi.org/10.1021/acs.molpharmaceut.8b00797.
[44] P. Chakravarty, J.W. Lubach, J. Hau, K. Nagapudi, A rational approach towards development of amorphous solid dispersions: experimental and computational techniques, Int. J. Pharm. 519 (2017) 44–57, https://doi.org/10.1016/J.IJPHARM.2017.01.003.
[45] D.J. Greenhalgh, A.C. Williams, P. Timmins, P. York, Solubility parameters as predictors of miscibility in solid dispersions, J. Pharm. Sci. 88 (1999) 1182–1190, https://doi.org/10.1021/JS9900856.
[46] A. Tihic, G.M. Kontogeorgis, N. von Solms, M.L. Michelsen, L. Constantinou, A predictive group-contribution simplified PC-SAFT equation of state: application to polymer systems, Ind. Eng. Chem. Res. 47 (2008) 5092–5101, https://doi.org/10.1021/ie0710768.
[47] J. Gross, G. Sadowski, Modeling polymer systems using the perturbed-chain statistical associating fluid theory equation of state, Ind. Eng. Chem. Res. 41 (2002) 1084–1093, https://doi.org/10.1021/ie010449g.
[48] R.J. Hemley, Effects of high pressure on molecules, Annu. Rev. Phys. Chem. 51 (2002) 763–800, https://doi.org/10.1146/annurev.physchem.51.1.763.
[49] M. Paluch, S.J. Rzoska, P. Habdas, J. Zio, On the isothermal pressure behaviour of the relaxation times for supercooled glass-forming liquids, 1998. https://iopscience.iop.org/article/10.1088/0953-8984/10/19/001/pdf (accessed April 5, 2019).
[50] Z.A. Worku, J. Aarts, G. Van den Mooter, Influence of compression forces on the structural stability of naproxen/PVP-VA 64 solid dispersions, Mol. Pharm. 11 (2014) 1102–1108, https://doi.org/10.1021/mp5001313.
[51] Z. Ayenew, A. Paudel, G. Van den Mooter, Can compression induce demixing in amorphous solid dispersions? A case study of naproxen–PVP K25, Eur. J. Pharm. Biopharm. 81 (2012) 207–213, https://doi.org/10.1016/j.ejpb.2012.01.007.
[52] Z. Wojnarowska, K. Adrjanowicz, P. Wlodarczyk, E. Kaminska, K. Kaminski, K. Grzybowska, R. Wrzalik, M. Paluch, K.L. Ngai, Broadband dielectric relaxation study at ambient and elevated pressure of molecular dynamics of pharmaceutical: indomethacin, J. Phys. Chem. B. 113 (2009) 12536–12545, https://doi.org/10.1021/jp905162r.
[53] I. Gutzow, B. Durschang, C. Russel, Crystallization of glassforming melts under hydrostatic pressure and shear stress: Part I Crystallization catalysis under hydrostatic pressure: possibilities and limitations, J. Mater. Sci. 32 (1997) 5389–5403, https://doi.org/10.1023/A:1018683331603.
[54] I. Gutzow, C. Russel, B. Durschang, Crystallization of glass forming melts under hydrostatic pressure and shear stress: Part II Flow induced melt crystallization: a new method of nucleation catalysis, J. Mater. Sci. 32 (1997) 5405–5411, https://doi.org/10.1023/A:1018635415674.
[55] J. Knapik-Kowalczuk, Z. Wojnarowska, M. Rams-Baron, K. Jurkiewicz, J. Cielecka-Piontek, K.L. Ngai, M. Paluch, Atorvastatin as a promising crystallization inhibitor of amorphous probucol: dielectric studies at ambient and elevated pressure, Mol. Pharm. 14 (2017) 2670–2680, https://doi.org/10.1021/acs.molpharmaceut.7b00152.
[56] M. Rams-Baron, J. Pacułt, A. Jędrzejowska, J. Knapik-Kowalczuk, M. Paluch, Changes in physical stability of supercooled etoricoxib after compression, Mol. Pharm. 15 (2018) 3969–3978, https://doi.org/10.1021/acs.molpharmaceut.8b00428.
[57] K. Chmiel, J. Knapik-Kowalczuk, K. Jurkiewicz, W. Sawicki, R. Jachowicz, M. Paluch, A new method to identify physically stable concentration of amorphous solid dispersions (I): case of flutamide + kollidon VA64, Mol. Pharm. 14 (2017) 3370–3380, https://doi.org/10.1021/acs.molpharmaceut.7b00382.
[58] K. Chmiel, J. Knapik-Kowalczuk, R. Jachowicz, M. Paluch, Broadband dielectric spectroscopy as an experimental alternative to calorimetric determination of the solubility of drugs into polymer matrix: case of flutamide and various polymeric matrixes, Eur. J. Pharm. Biopharm. 136 (2019) 231–239, https://doi.org/10.1016/j.ejpb.2019.01.025.
[59] J. Knapik-Kowalczuk, K. Chmiel, K. Jurkiewicz, Z. Wojnarowska, M. Kurek, R. Jachowicz, M. Paluch, Influence of polymeric additive on the physical stability and viscoelastic properties of aripiprazole, Mol. Pharm. 16 (2019) 1742–1750, https://doi.org/10.1021/acs.molpharmaceut.9b00084.
[60] M. Romanini, M. Lorente, B.S. Schammé, L. Delbreilh, V.V. Dupray, G.G. Coquerel, J. Lluís Tamarit, R. Macovez, Enhancement of the physical and chemical stability of amorphous drug − polymer mixtures via cryogenic comilling, Macromolecules (2018), https://doi.org/10.1021/acs.macromol.8b01271.
[61] J.A. Baird, L.S. Taylor, Evaluation of amorphous solid dispersion properties using thermal analysis techniques, Adv. Drug Deliv. Rev. 64 (2012) 396–421, https://doi.org/10.1016/j.addr.2011.07.009.
[62] G. Van den Mooter, M. Wuyts, N. Blaton, R. Busson, P. Grobet, P. Augustijns, R. Kinget, Physical stabilisation of amorphous ketoconazole in solid dispersions with polyvinylpyrrolidone K25, Eur. J. Pharm. Sci. 12 (2001) 261–269, https://doi.org/10.1016/S0928-0987(00)00173-1.
[63] M. Gordon, J.S. Taylor, Ideal copolymers and the second-order transitions of synthetic rubbers. i. non-crystalline copolymers, J. Appl. Chem. 2 (1952) 493–500, https://doi.org/10.1002/JCTB.5010020901.
[64] M. Rams-Baron, Z. Wojnarowska, K. Grzybowska, M. Dulski, J. Knapik, K. Jurkiewicz, W. Smolka, W. Sawicki, A. Ratuszna, M. Paluch, Toward a better understanding of the physical stability of amorphous anti-inflammatory agents: the roles of molecular mobility and molecular interaction patterns, Mol. Pharm. 12 (2015) 3628–3638, https://doi.org/10.1021/acs.molpharmaceut.5b00351.
[65] J. Knapik, Z. Wojnarowska, K. Grzybowska, K. Jurkiewicz, A. Stankiewicz, M. Paluch, Stabilization of the amorphous ezetimibe drug by confining its dimension, Mol. Pharm. 13 (2016) 1308–1316, https://doi.org/10.1021/acs.molpharmaceut.5b00903.
[66] F. Kremer, A. Schönhals, Broadband Dielectric Spectroscopy, 2003. https://doi.org/10.1007/978-3-642-56120-7.
[67] H. Vogel, Temperaturabhangigkeitgesetz der Viskosität von Flüssigkeiten, J. Phys. Z (1921) 645–646 https://scholar.google.pl/scholar?hl=pl&as_sdt=0%2C5&q=Vogel+H.%3B+J.+Phys.+Z.+1921%2C+22%2C+645−646&btnG=&oq=J+phys+Z (accessed October 3, 2017).
[68] G.S. Fulcher, Analysis of recent measurements of the viscosity of glasses, J. Am. Ceram. Soc. 8 (1925) 339–355, https://doi.org/10.1111/j.1151-2916.1925.tb16731.x.
[69] G. Tammann, W. Hesse, Die Abhängigkeit der Viscosität von der Temperatur bie unterkühlten Flüssigkeiten, Zeitschrift Für Anorg. Und Allg. Chemie. 156 (1926) 245–257, https://doi.org/10.1002/zaac.19261560121.
[70] A. Prudic, T. Kleetz, M. Korf, Y. Ji, G. Sadowski, Influence of copolymer composition on the phase behavior of solid dispersions, Mol. Pharm. 11 (2014) 4189–4198, https://doi.org/10.1021/mp500412d.
[71] A. Prudic, Y. Ji, G. Sadowski, Thermodynamic phase behavior of API/polymer solid dispersions, Mol. Pharm. 11 (2014) 2294–2304, https://doi.org/10.1021/mp400729x.
[72] J. Knapik-Kowalczuk, Z. Wojnarowska, K. Chmiel, M. Rams-Baron, L. Tajber, M. Paluch, Can storage time improve the physical stability of amorphous pharmaceuticals with tautomerization ability exposed to compression? The case of a chloramphenicol drug, Mol. Pharm. (2018), https://doi.org/10.1021/acs.molpharmaceut.8b00099.
[73] K. Adrjanowicz, K. Kaminski, Z. Wojnarowska, M. Dulski, L. Hawelek, S. Pawlus, M. Paluch, W. Sawicki, Dielectric relaxation and crystallization kinetics of ibuprofen at ambient and elevated pressure, J. Phys. Chem. B. 114 (2010) 6579–6593, https://doi.org/10.1021/jp910009b.
[74] C.M. Roland, S. Hensel-Bielowka, M. Paluch, R. Casalini, Supercooled dynamics of glass-forming liquids and polymers under hydrostatic pressure, Reports Prog. Phys. 68 (2005) 1405–1478, https://doi.org/10.1088/0034-4885/68/6/R03.
[75] S. Hensel-Bielowka, S. Pawlus, C.M. Roland, J. Zioło, M. Paluch, Effect of large hydrostatic pressure on the dielectric loss spectrum of type- a glass formers, Phys. Rev. E 69 (2004) 050501, https://doi.org/10.1103/PhysRevE.69.050501.